Jurnal Teknologi

Full paper

The Effect of Steel Yielding on CFRP Plated Steel Member by Partial Interaction Theory

Ibrisam Akbar[a*], Deric Oehlers[b], Mohamed Ali Sadakkathulla[a]

[a]*Civil Engineering Department, Universiti Teknologi PETRONAS, Bandar Seri Iskandar, 31750 Tronoh, Perak, Malaysia*
[b]*School of Civil Environmental and Mining Engineering, Faculty of Engineering, Computer & Mathematical Sciences Level 1, Ingkarni Wardli, The University of Adelaide SA 5005, Australia*

*Corresponding author: ibrisam_akbar@petronas.com.my

Article history

Received :1 November 2012
Received in revised form :15 January 2013
Accepted :15 March 2013

Graphical abstract

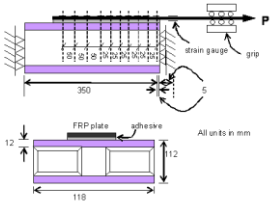

Abstract

The reliability in strengthening concrete or steel structures using Carbon Fibre Reinforced Polymer (CFRP) depends on the success of the stress transfer between the two materials. This paper presented a simple numerical approach to simulate the stress transfer by applying partial interaction theory. The numerical approach uses a local bond-slip (τ-δ) model obtained from a previous experimental work. Pull tests were conducted on a dog-bone shaped steel specimens to initiate yielding of the steel. Results from the tests and published data compared with the numerical values show good correlations. These provide useful insights in the existence of full and partial interaction regions along the bonded length of the CFRP.

Keywords: Cfrp; frp; strengthening; steel; bond-slip

Abstrak

Kebolehpercayaan dalam pengukuhan struktur konkrit atau keluli menggunakan Polimer Bertetulang Gentian Karbon (CFRP) bergantung kepada kejayaan pemindahan tegasan antara kedua-dua bahan tersebut. Kertas kerja ini membentangkan satu pendekatan berangka yang mudah untuk mensimulasikan pemindahan tegasan dengan menggunakan teori interaksi separa. Pendekatan berangka menggunakan model tempatan ikatan-gelincir (τ-δ) yang diperolehi dari kerja eksperimen sebelumnya. Ujian tarikan telah dijalankan ke atas spesimen keluli berbentuk tulang-anjing untuk memulakan alahan keluli. Korelasi yang baik dapat diperhatikan dari perbandingan antara keputusan ujian ini dan keputusan ujian lepas jika dibandingkan dengan kaedah berangka. Ini memberikan pandangan yang berguna dalam kewujudan kawasan interaksi penuh dan separa sepanjang panjang ikatan CFRP.

*Kata kunci:*Cfrp; frp; gentian karbon terkukuh polimer; keluli

1.0 INTRODUCTION

The ease of use, the high stiffness-to-weight and strength-to-weight ratios combined with the superior environmental durability has made Carbon Fibre Reinforced Polymer (CFRP) so appealing to be used in the area of strengthening and retrofitting [**1**]. However, the reliability of the strengthening of CFRP to steel or concrete structures depends on the success of the stress transfer between the CFRP plate and steel or concrete element [2, 3] and one of the critical stage is to understand the bond-slip characteristics of CFRP plated steel members which is susceptible to the yielding of the steel. Although considerable amount of research has been conducted on the interaction of steel-CFRP, a few of them touches on the effect of steel yielding [4].

2.1 Bond-Slip Relationship

Bond-slip (τ-δ) relationship plays an important role in characterizing the behavior of CFRP bonded steel. It is used to obtain bond strength, slip, and an effective bond length. An accurate local bond-slip (τ-δ) model is important in the modeling of FRP-strengthened RC structures [5]. The problem of violent variations in the strain readings in the CFRP-concrete experiment can be eliminated by replacing the concrete with steel [6]. Various bond-slip models were suggested and out of these, the experimental results indicated that the bilinear model provides the close approximation [4, 7, 8]. Experimentally, the values of the τ-δ are obtained in pull tests as shown in Figure 1. The bilinear τ-δ relationship is explained where the maximum bond stress, τ_{max}, the maximum slip, δ_{max} and the slip at the maximum bond stress, δ_1 are marked in Figure 2. The fracture energy, G_f, is the area encompassed by the τ_{max}-δ_{max}. As long as the values of τ_{max}-δ_{max} are constant, G_f does not change since the

area under it does not change. Similarly, when calculating a unilinear relationship where δ_1 is equal to *0*, G_f does not change as well.

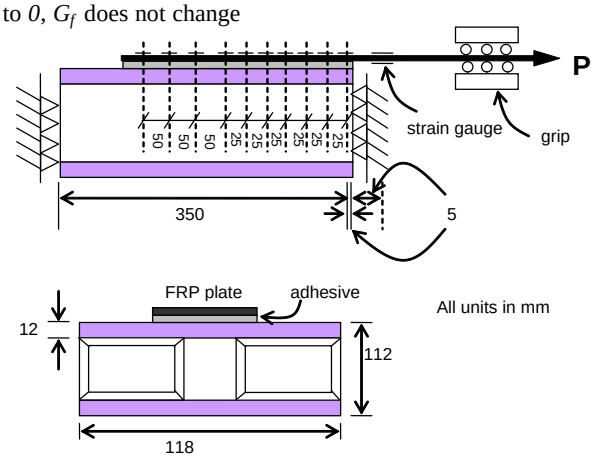

Figure 1 Pull test specimen.

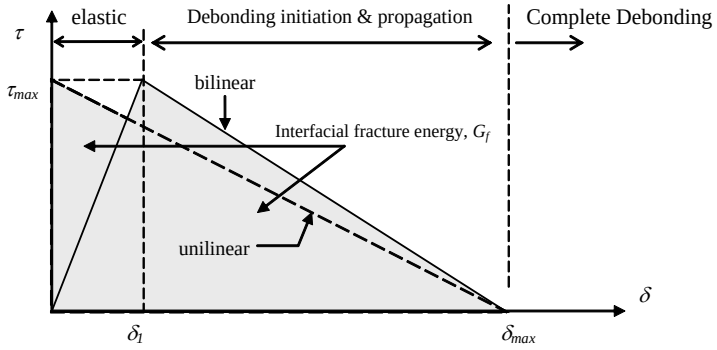

Figure 2 Bilinear bond-slip relationship

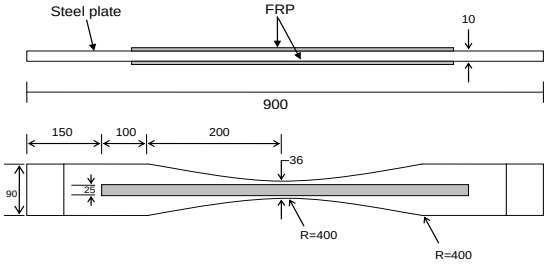

(a) Test specimen

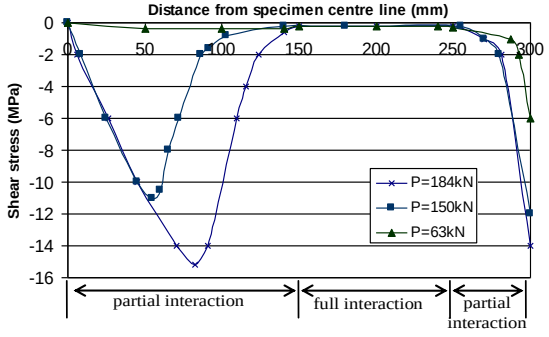

(b) Finite element stress distributions

Figure 3 Dog-bone Specimen and finite element results

2.2 Past Experiments

Pull test were conducted where 13 specimens were tested as shown in Figure 1 [**7**]. It consists of a steel block with bonded with CFRP plate. Strain gauges were glued along the bonded length so that the slip can be measured. The average bond stresses were calculated from the readings of the strain gauges upon the intervals of each strain gauge. By integrating the measured strain obtained from the strain gauges glued at the CFRP plate length, the slip can be determined. However, the strain gauges can only give average stresses and can miss the peak stresses. The readings may be affected by local distortion of the plate whilst debonding since the strain gauges are only placed on the outer surface of the CFRP plate. Furthermore, the experiment is costly with the amount of strain gauges attached to the CFRP plate and exhaustive. The improvement in obtaining the τ-δ relationship in CFRP-concrete using structural mechanics method was conducted [**9**].

A dog-bone pull tests were conducted to investigate the bond behaviour of CFRP plated steel member as shown in Figure 3 [**10**]. It shows that debonding may occurs at the middle section where the steel has yielded as shown in Figure 3(b) rather than at the plate end. Based on the finite element analysis conducted in the same research, it was found that there were possibilities of full and partial interaction region to exist on the plated system. The significance of this findings are (a) the full interaction region is not critical and does not need as much attention as the plate end and middle regions and (b) it may affect on how CFRP is used for the strengthening of steel members.

For the purpose of demonstrating plate end debonding, a constant width steel plate glued with CFRP plate has been reported [**11**]. By varying the FRP bonded length, it was shown that the existence of high bond stress at the plate end translate into debonding no matter what is the bonded length. Excess of the critical bond length measured from the plate end is not going to be affected.

2.0 NUMERICAL METHOD

The partial interaction numerical method developed earlier [**6**] is modified for this purpose. The dog-bone specimen in Figure 4 (a) is simplified as in Figure 4 (b) due to symmetry. The idealisation should be able to accommodate any local failure plane (L_{per}) and τ-σ relationship, bonded length (L), cross section of the steel (A_s) and CFRP (A_p) and stress-strain profile of the steel plate and CFRP (which includes the Young's Modulus of the steel and CFRP, E_s and E_p respectively) [**12**].
The numerical procedures are as follows:

- Strain of steel is fixed at the middle $\varepsilon_s(0)$ and the strain of CFRP, $\varepsilon_p(0)$ is guessed.
- According to the stress-strain profile of the steel and CFRP, the load at the centre, $P_s(0)$ and $P_p(0)$ are calculated.
- The load in the steel and CFRP are calculated at the end of the first segment : $P_s(0)=\varepsilon_s E_s t_s L_{per}$ and $P_p(0)=\varepsilon_p E_p t_p b_p$.
- Due to symmetry at the centre, slip at this section is zero.
- The assumed slip at the centre corresponds to the local slip over the first segment length. Corresponding to this assumed slip, $\delta(0)$, the bond stress, $\tau(0)$, acting over the first segment length is calculated according to the local τ-σ relationship assumed.
- The bond force acting on the first segment is $B(0)=\tau(0)d_x b_b$.
- The load in the steel and CFRP is calculated at the end of the first segment : $P_s(1)=P_s(0)+B(0)$ and $P_p(1)=P_p(0)-B(0)$,
- The corresponding strain for the steel and CFRP are calculated: $\varepsilon_s(1)=\frac{P_s(1)}{(A_s E_s)}$ and $\varepsilon_p(1)=\frac{P_p(1)}{(A_p E_p)}$
- The slip strain is calculated: $\frac{ds(0)}{dx}=\varepsilon_s(0)-\varepsilon_p(0)$
- The change in slip over the first segment length is calculated by integrating the slip strain over the segment length: $\Delta s(0)=\int \frac{ds(0)}{dx}dx$.
- According to the change in slip over the segment length, the slip at the beginning of the second segment is calculated: $\delta(1)=\delta(0)-\Delta s(0)$.
- According to this slip the bond force acting over the second segment is calculated, with the numerical process repeating itself over the subsequent segments.
- If the boundary condition is not met, then change the assumed $\varepsilon_p(0)$. If the boundary condition is met, then increase the fixed $\varepsilon_s(0)$.

Figure 5 further illustrates the boundary conditions of the numerical procedure for the solution to be met using the partial interaction theory. Consider the partial interaction region at the right side of the figures. The length of this region is based on the critical bond length, L_{crit} which is defined as the minimum bond length required such that the peak debonding load is attained [9]. Once the critical bond length has been achieved, a full interaction region will exist which has been reported elsewhere [11] where only plate end debonding is considered. If yielding of steel is considered on the left side of Figure 5, then another partial interaction region will exist due to difference of strains between the steel and CFRP. As yielding is occurring at a specific length, the full interaction will remains in its variable length depending on how long is the bonded length. Solution for the numerical procedure in Figure 5 can be found at the partial interaction regions on left and right. First, the point where the *slip=slipstrain=0* at the partial interaction region on the left side of Figure 5 which is the subject of this paper. The second numerical solution is at the partial interaction region on the right side which is reported elsewhere [11].

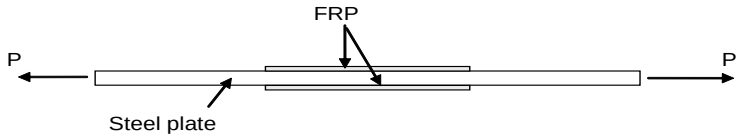

(a) laboratory specimen

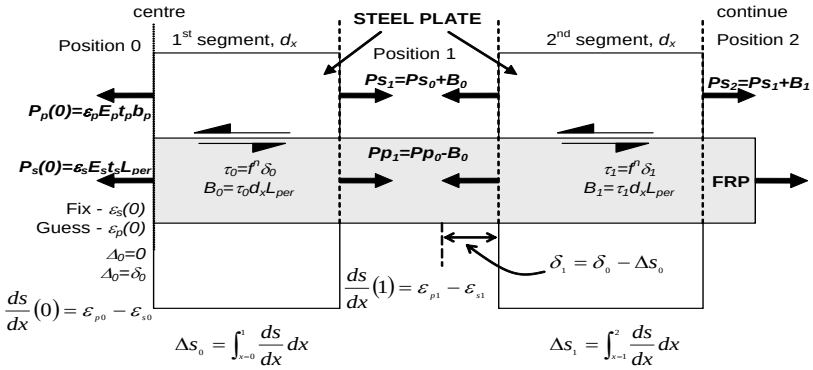

(b) numerical idealisation

Figure 4 Graphical representation of the numerical analysis for CFRP plated steel members

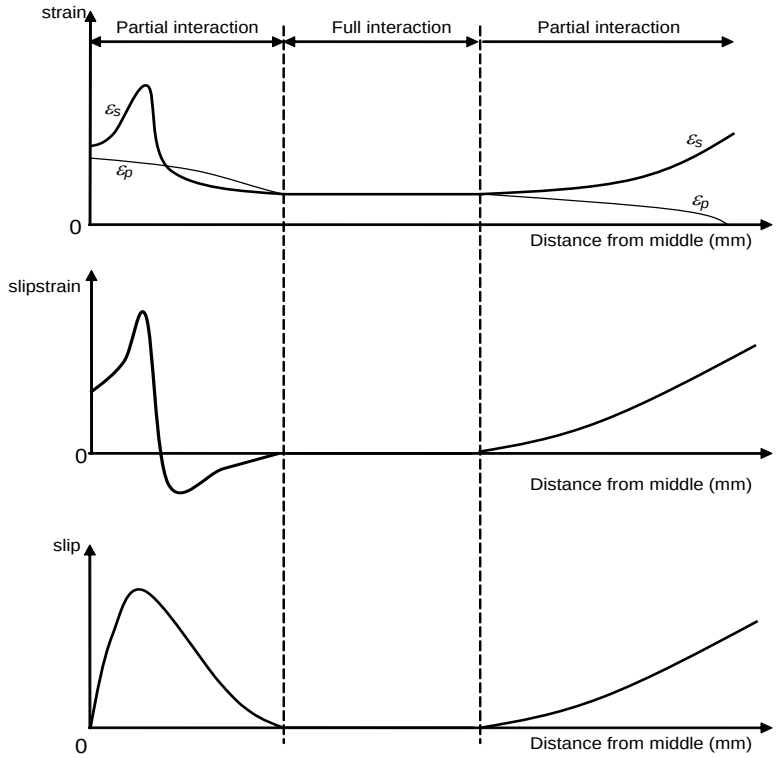

Figure 5 Full and partial interaction regions of CFRP plated steel member.

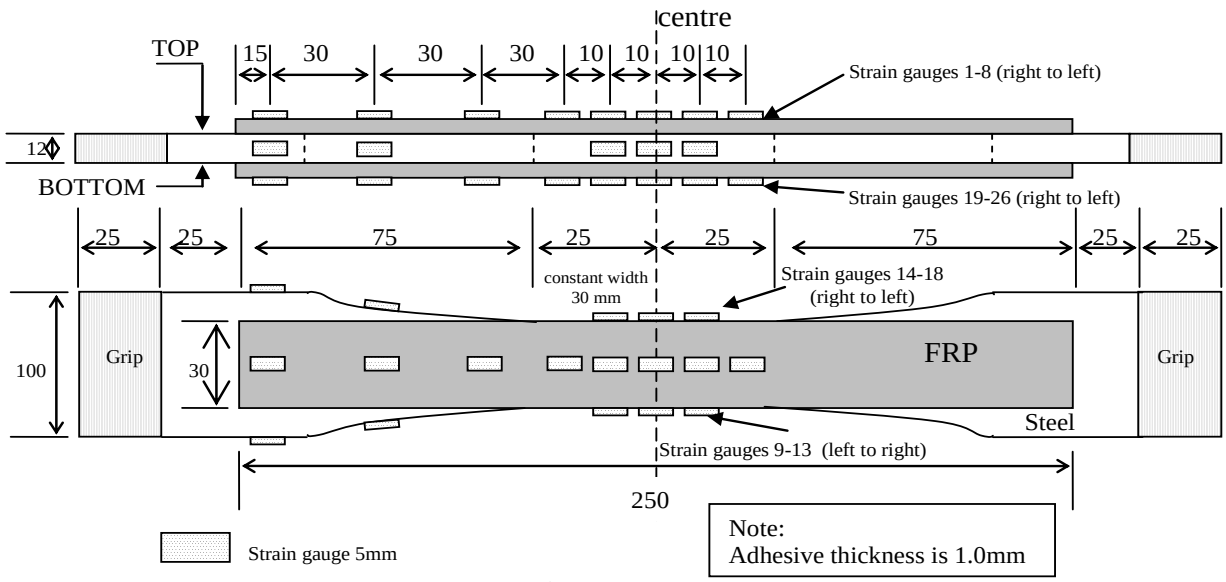

Figure 6 Shape and dimension of dog-bone specimen with strain gauge locations.

■3.0 SPECIMEN PREPARATION AND TEST PROCEDURE

The shape and dimension of the specimen to be tested is shown in Figure 6. The steel plate was varied in width from 100 mm at the widest to 30 mm at the thinnest. The tapered section was prepared so that yielding of steel can be achieved at the middle section. The constant width of 30 mm that ran for 50 mm in length was designed to provide spaces for strain gauges to be glued. The concentration of the strain gauges at the middle section is more since it is the region of study. Based on calculation, the bonded length of 250 mm has achieved its critical bond length and is applied in the specimen. The thickness of the CFRP plate is 1.2 mm. Two specimens were prepared based on previous experiment [10]; one with a single layer of CFRP and the other with two layers of CFRP.

Steel surfaces (top and bottom) were sandblasted to enhance the bonding capability and cleaned with acetone to remove any dirt, rust and residues. The adhesive consisted of two parts; A and B which were mixed in the ratio of 1:1. After mixing, there was about 45 minutes for the adhesive to be applied on to the steel block before it became too sticky to be workable. The thickness of adhesive was set approximately 1mm thick by using a 1 mm diameter ball bearing which was glued to the steel surface with a layer of adhesive to keep it even along the bonded length. Then, a sufficient force (a weight of 20 kg) is placed on top of the CFRP plate for a minimum of five hours so that constant thickness of adhesive can be achieved and any excess adhesive out from the CFRP plate can be removed.

Curing was done for five days. Following that, strain gauges were glued on the CFRP and steel surfaces to monitor the longitudinal strain at the middle section. The overall geometrical properties for the specimens are tabulated in Table 1.For the steel material properties, three tension pull tests were conducted on the steel plate to get the stress-strain relationship as tabulated in Table 2. The specimens were then tested on a Universal Testing Machine (UTM).

Table 1 Specimen properties

Test specimen	Steel thickness, t_s (mm)	CFRP width, b_p (mm)	CFRP layer	Bonded length, L_p (mm)
VW 1	11.95	30.0	1	250
VW 2	11.96	30.0	2	250

Table 2 Material properties of the steel plate

Test specimen	Averaged
Yield load, P_y (kN)	115.9
Yield stress, f_y (MPa)	308
Yield strain, ε_Y	0.00152
Young's Modulus, E_s (MPa)	202348
Strain hardening stress, f_{sh} (MPa)	473
Strain hardening, ε_{sh}	0.078

■4.0 TEST RESULTS

The debonding failures were a mix of FRP layer, steel-adhesive layer and CFRP-adhesive layer. At the top surface as shown in Figure 7 (a), the debonding failure occurred on the CFRP-adhesive layer failure mainly occurred close to the plate end, whereas, steel-adhesive layer at the middle part of the steel plate. At the bottom surface as shown in Figure 7 (b), the debonding failure occurs at the plate end debonding occurred at the CFRP-adhesive and within the FRP, whereas, layers at the steel-adhesive layer in the middle of the specimen. The FRP did

not break or split. The steel plate breaks only after the CFRP has been totally debonded.

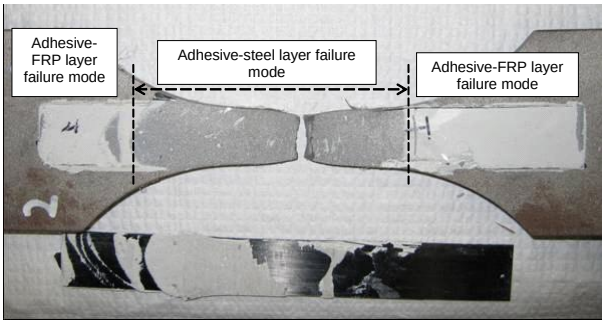

(a) top surface

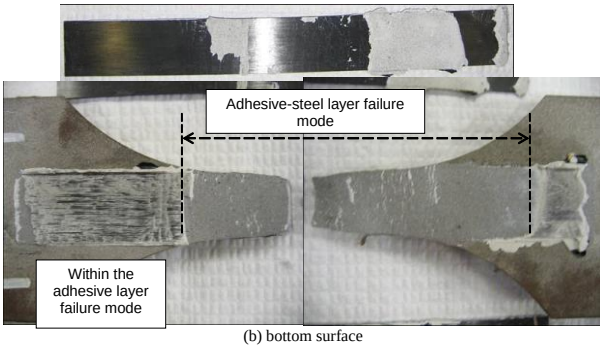

(b) bottom surface

Figure 7 Failure mode of specimen VW1

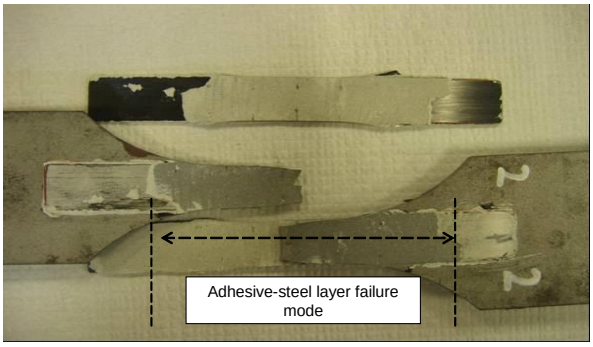

(a) top surface

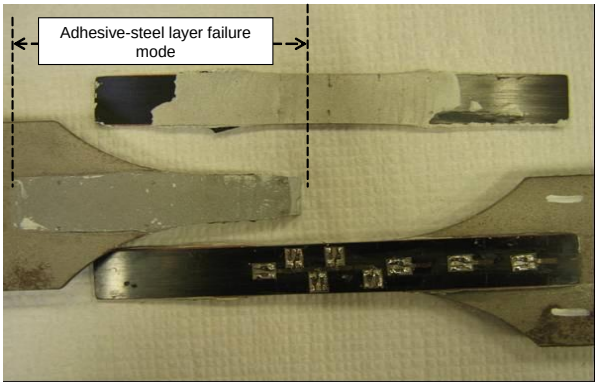

(b) bottom surface

Figure 8 Failure mode of specimen VW2

Two layers of CFRP were bonded on sample VW2. The rest of the experimental setup was the same as in sample VW1. Figure 8 shows the specimen at failure. At the top surface, the debonding at the steel-adhesive layer occurred at the middle section and debonding at the CFRP-adhesive layer at the plate end. At the bottom surface, only one side has been debonded, mainly at the steel-adhesive layer.

It is clear from the visual inspection of the failures that the debonding occurs at the steel-adhesive layer at the region where steel yielding is initiated and CFRP-adhesive at the plate end. This is because the ductility of the steel allows huge steel strain increment after reaching the yield point. At the same time the brittle nature of adhesive does not allow the same strain increment, hence debonding is allowed at the steel-adhesive layer. However, CFRP is also brittle at the plate end and since the yielding of steel is unlikely to occur at the plate end, the failure will occur at the CFRP-adhesive, within CFRP or within adhesive layer, depending on the material properties of both materials.

The three stages of behaviour prior to failure; linear-elastic, steel yielding and debonding, were clearly illustrated in load-strain curve of specimen VW1 and VW2 as shown in Figure 9 and Figure 10. Readings were taken at the middle point of the specimen. As steel has yielded, the strain increased rapidly at a small increase of load. This is the stage where debonding has been initiated. At debonding stage, no increase of load can be resisted anymore and the CFRP was debonded. Once debonding has occurred, the total debonding of the CFRP occurred rapidly which explains the sudden drop in the graphs. Although there are no significant difference in the debonding failure load between VW1 and VW2, the numerical values show that with the increment of CFRP layer in VW2, the strain value at failure is lower. The description of the failure mode in Figure 9 and Figure 10 is in consistence with the bilinear τ-δ relationship as described in Figure 2.

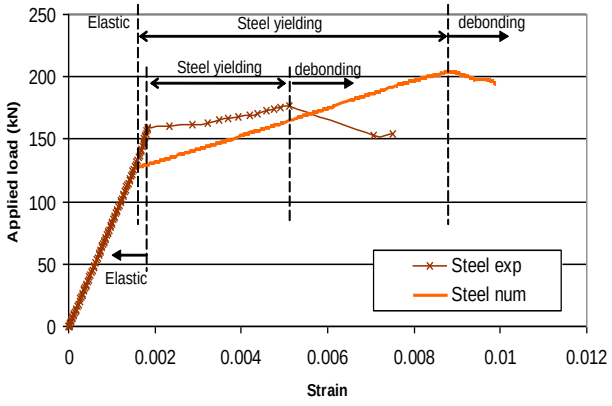

Figure 9 Steel load-strain comparison for VW1

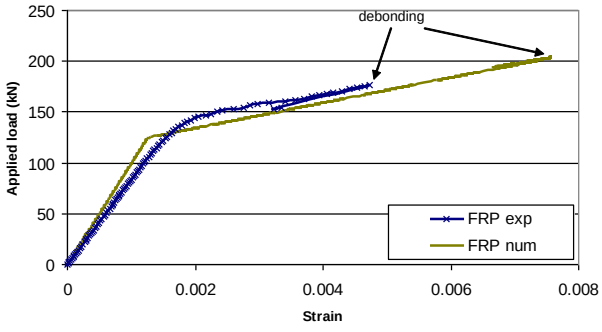

Figure 10 CFRP load-strain comparison for VW2

5.0 ANALYSIS OF TEST RESULTS

The debonding of CFRP plated steel when steel has yielded is explained in this section. The values of the τ_{max} and δ_{max} are 22.9 MPa and 0.2 mm respectively and the value for δ_1 is 0.1 mm were obtained from previous research using the same types of adhesive and CFRP plate [**6**]. Infinite bonded length was used in the numerical method but the length of the area where the steel is allowed to yield is set to follow the experimental specimen. Once the steel has yielded, the slip increased drastically. Figure 11 shows the slip development of specimen VW1. At linear-elastic stage, the slip development is very low throughout the bonded length. Similarly, the bond stress in Figure 12 shows very low values throughout the bonded length. When the steel has yielded, a significant increase of slip is observed in Figure 11 at 0.1 mm which is also the value of δ_1. The corresponding bond stress in Figure 12 shows that the bond stress has reached its peak (the ascending branch of the τ-δ relationship in Figure 2).

At debonding, which is defined when the value of δ_{max} has been exceeded, in this case 0.22 mm, the corresponding bond stress is described in Figure 12. Debonding occurs about 24 mm to 43 mm from the middle section. To the left and right of the debonded length, descending branch of the τ-δ relationship in Figure 2 is observed and peaked at the specified τ_{max} value of 22.9 MPa. The ascending branch follows after reaching the τ_{max}. As the debonding area propagates to the left and right, the τ_{max} will also shifted further to the left and right until the whole bonded length has debonded. However, when full interaction exist due to the high strain increment of the yielding of steel, the debonding will only occur at the partial interaction region as described earlier, until the steel breaks, leaving a scenario where the CFRP is still attached to the steel plate at the full interaction area. This can be observed in Figure 8 (a) where the CFRP is still attached to the steel plate.

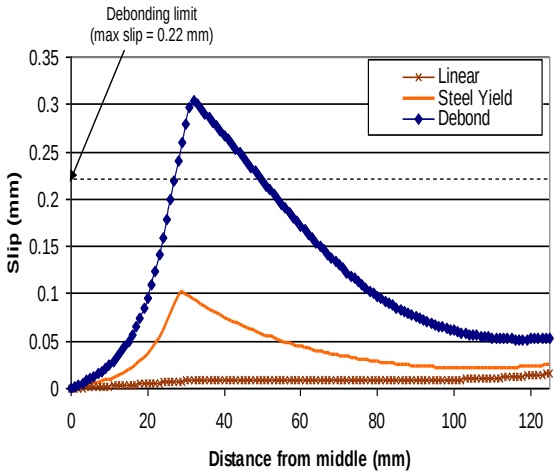

Figure 11 Numerical slip at different stages of loading (VW1)

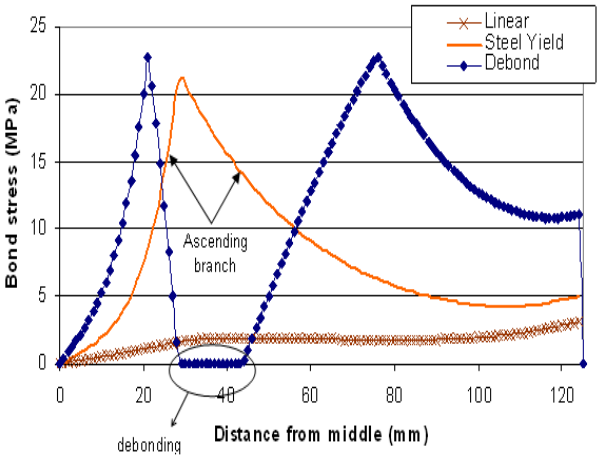

Figure 12 Numerical bond stress at different stages of loading (VW1)

6.0 APPLICATION OF NUMERICAL METHOD

In this section, the application of the numerical method is validated with a published result where similar dog-bone steel plate specimens were tested with varying layers of CFRP [**10**]. In the research, 13 specimens were tested. The τ-δ relationship was not available from the published reports hence a generic values similar to the current research were applied for the τ_{max}, δ_{max} and δ_1. Due to this, it is important to note that in this comparison, the accurateness of the resulting values are not as important as the debonding mechanism described by the following comparison of experimental and numerical values.

Two specimens from the published reports were compared, A12 and B17 which have different types of adhesive and CFRP thicknesses. Experimental and FEM results of the published report are reproduced in this section. Figure 13 shows the comparison of load-axial stress of the steel plate. The experimental results were based on the strain readings on the CFRP plate at the middle of the section and compared with the numerical results develop in the current research. From the visual inspection, specimen A12 failed due to debonding in the middle of specimen after the steel plate yielded. In the numerical analysis, the decrease of the CFRP stresses as shown in Figure 13 after the steel has yielded suggesting that the successive yielding of steel leads to the debonding which is also the type of failure occurred on sample VW1. The numerical curve follows the experimental curve quite closely as the steel plate has yielded and after taking more load, both failed at a peak applied load between 185 kN to 200 kN.

The stress recorded by the numerical analysis for specimen B17 (Figure 14) was 1106 MPa prior to debonding in contrast to 1384 MPa from the experiment which exceeded the ultimate tensile stress of 1252 MPa. Since the ultimate tensile strength has been exceeded, the CFRP ruptured instead of debonding. A close proximity of the ultimate value from the numerical method compare to the ultimate tensile stress and the no-solution found in the iteration suggested a similar CFRP rupture failure.

Figure 15 shows the bond stress distribution along the bonded length from the experiment and numerical for specimen A12. At 150 kN (149 kN for the numerical analysis), the steel plate has yielded, creating a high bond stress at the middle of the specimen. It was suggested that the debonding may occur first at the middle section before at the plate end based on the high bond stress which also occurred at the plate end. In the numerical analysis as shown in Figure 15 (b), it is suggested that

debonding occurred at the middle section and then propagates toward the plate end as indicated by the debonding propagation of specimen VW1. In essence, the numerical computation in Figure 15 (b) shows a good behavioural correlation to FEM in Figure 15 (a) despite not knowing the exact material properties of the materials used.

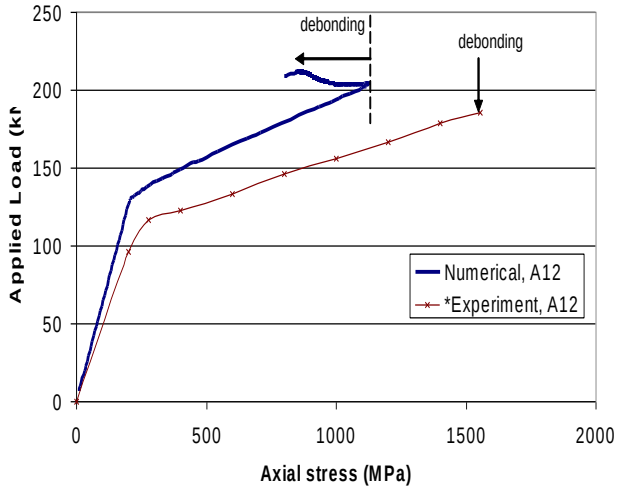

Figure 13 Numerical and experimental load-axial stress comparison for specimen A12

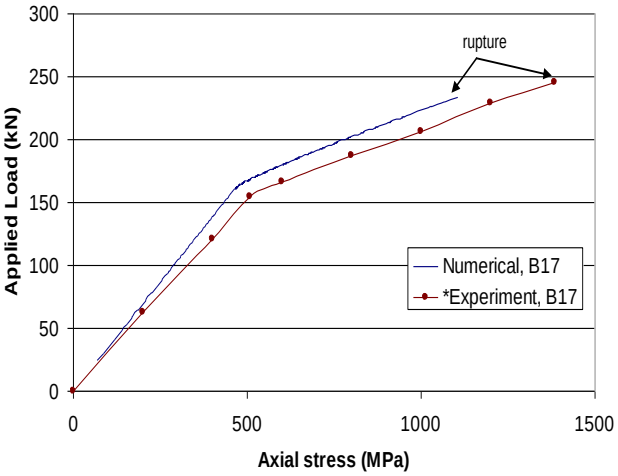

Figure 14 Numerical and experimental load-axial stress comparison for specimen B17

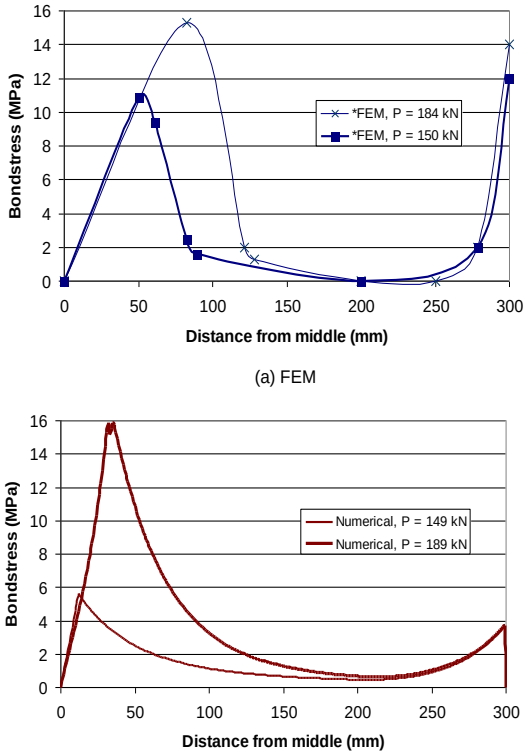

Figure 15 Numerical and FEM shear stress comparison across the bonded length (specimen A12)

7.0 CONCLUSION

The numerical method developed in this paper, using the partial interaction theory has been proven to shows relatively good correlations with the experimental and FEM results. The numerical method has been able to interact with the τ-δ relationship and then calculating the strains and stresses at the linear-elastic, yielding and debonding stages. Using the numerical method, it is found that high stress which leads to debonding in the case of dog-bone steel-CFRP specimen may occur at the region where the steel is allowed to yield, backed by the experimental and FEM results. Further works by varying the types of CFRP, steel and adhesive are essential in order to postulate a generic behaviour of the material interactions.

Acknowledgement

The authors would like to extend their acknowledgement to the Universiti Teknologi PETRONAS and The University of Adelaide for providing the funding and resources for the accomplishments of this research study.

References

[1] Buyukozturk, O., Gunes, O. and Karaca, E. 2003. Progress on Understanding Debonding Problems in Reinforced Concrete and Steel Members Strengthened Using FRP Composites. *Construction and Building Materials*. 18(1): 9–19.

[2] Al-Saidy, A. H., Klaiber, F. W. and Wipf, T. J. 2005. Strengthening of Steel–Concrete Composite Girders Using Carbon Fiber Reinforced Polymer Plates. *Construction and Building Materials*. 21(2): 295–302.
[3] Sebastian, W. M. 2003. Nonlinear Proportionality of Shear-Bond Stress to Shear Force in Partially Plastic Regions of Asymmetric FRC-Laminated Steel Members. *International Journal of Solids and Structures*. 40(1): 25–46.
[4] Zhao, X.-L. and Zhang, L. 2007. State-Of-The-Art Review on FRP Strengthened Steel Structures. *Engineering Structures*. 29(8): 1808–1823.
[5] Lu, X. Z., Teng, J. G., Ye, L. P. and Jiang, J. J. 2005. Bond–Slip Models For FRP Sheets/Plates Bonded to Concrete. *Engineering Structures*. 27(6): 920–937.
[6] Akbar, I., Oehlers, D. J. and M. S., M. A. 2010. Derivation of the Bond-Slip Characteristics for FRP Plated Steel Members. *Journal of Constructional Steel Research*. 66(8-9): 1047–1056
[7] Xia, S. H. and Teng, J. G. 2005. Behaviour of FRP-To-Steel Bonded Joints. International Institute for FRP in Construction. Hong Kong.
[8] Yuan, H., Teng, J. G., Seracino, R., Wu, Z. S. and Yao, J. 2004. Full-Range Behavior of FRP-To-Concrete Bonded Joints. *Engineering Structures*. 26(5): 553–565.
[9] Haskett, M., Oehlers, D. J. and Ali, M. S. M. 2007. Local and Global Bond Characteristics of Steel Reinforcing Bars. *Engineering Structures*. 30(2): 376–383.
[10] Al-Emrani, M. and Kliger, R. 2006 Experimental and Numerical Investigation of the Behaviour and Strength of Composite Steel-CFRP Members. *Advances in Structural Engineering*. 9(6): 819–831.
[11] Akbar, I., Oehlers, D. J. and Ali, M. S. M. 2010. Partial and Full Interaction Behaviour of FRP Plated Steel Member. *International Conference on Sustainable Building and Infrastucture*. Kuala Lumpur.
[12] Seracino, R., Raizal Saifulnaz, M. R. and Oehlers, D. J. 2007. Generic Debonding Resistance of EB and NSM Plate-To-Concrete Joints. *Composite for Constructions*. 11(1): 62–70.